

## PROSPECTS FOR THE DETECTION OF THE DEEP SOLAR MERIDIONAL CIRCULATION

D. C. BRAUN AND A. C. BIRCH

NorthWest Research Associates, CoRA Division, 3380 Mitchell Lane, Boulder, CO 80301; dbraun@cora.nwra.com, aaronb@cora.nwra.com  
Received 2008 October 1; accepted 2008 October 28; published 2008 November 14

### ABSTRACT

We perform helioseismic holography to assess the noise in  $p$ -mode travel-time shifts which would form the basis of inferences of large-scale flows throughout the solar convection zone. We also derive the expected travel times from a parameterized return (equatorward) flow component of the meridional circulation at the base of the convection zone from forward models under the assumptions of the ray and Born approximations. From estimates of the signal-to-noise ratio for measurements focused near the base of the convection zone, we conclude that the helioseismic detection of the deep meridional flow including the return component may not be possible using travel-time measurements spanning an interval less than a solar cycle. We speculate that this conclusion may be generally true for other helioseismic methods under the assumption that the underlying measurements are equivalently limited by solar realization noise.

*Subject headings:* Sun: helioseismology — Sun: interior

### 1. INTRODUCTION

Among all known large-scale flows in the Sun, the meridional circulation has particular significance because of its role in the transport of angular momentum and magnetic flux across a wide range of latitudes within the convection zone. Consequently, it is a significant component of models of the dynamics of rotating stellar convection zones, dynamos, and the solar cycle (e.g., Glatzmaier & Gilman 1982; Choudhuri et al. 1995; Wang et al. 1991; Hathaway et al. 2003; Dikpati & Gilman 2007).

Measurements of the surface manifestation of meridional circulation have typically indicated poleward flows between 10 and 20 m s<sup>-1</sup> (e.g., Hathaway 1996; Schou 2003). Although frequencies of global  $p$ -modes are insensitive (to first order) to the meridional circulation, the flows have been detected with a variety of local seismic methods (e.g., Giles et al. 1997; Braun & Fan 1998; González Hernández et al. 1999; Haber et al. 2002; Hughes & Thompson 2003; Zhao & Kosovichev 2004; Chou & Ladenkov 2005; Roth & Stix 2008). Many of these studies have focused their attention on the meridional circulation near the surface (e.g., within a few tens of Mm below the surface), and only a few attempts have been made to deduce the properties of the deeper components. Among the most comprehensive analyses is the work of Giles (2000) which is based on models of time-distance measurements using over 2 years of Michelson Doppler Imager (MDI; Scherrer et al. 1995) Dopplergrams. These models included two general solutions for the meridional circulation as a function of depth and latitude: the first (hereafter “Giles’ model A”) without any constraint on mass conservation, and the second (Giles’ model B) with an imposed mass conservation. Only Giles’ model B exhibited a return flow while the other showed exclusively poleward flows throughout the convection zone. Each model was consistent with the travel-time measurements within their range of errors (Giles 2000).

In the frequency-wavenumber range of  $p$ -modes propagating through the bottom half of the convection zone, the random noise present in most current helioseismic measurements is dominated by realization noise caused by stochastic excitation of the  $p$ -modes near the solar surface. For the exploration of large-scale flows such as meridional circulation this could be reduced by observing more of the Sun (e.g., the far side of the

Sun which is not currently accessible to helioseismic instruments) or by employing data sets with longer temporal duration. With over a decade of helioseismic observations from both the Global Oscillations Network Group (GONG) and MDI now available,<sup>1</sup> it is worthwhile to revisit the issue of the deep meridional circulation. In this Letter, we explore the prospects for helioseismic detection of the return component of the meridional circulation in the deep solar convection zone by applying helioseismic holography to MDI observations to assess the random noise in travel-time shifts which would form the basis for the inference of large-scale flows. Our analysis and resulting noise estimates are described in § 2. We estimate the expected signal from a plausible return component of meridional circulation using forward modeling procedures described in § 3. This is followed in § 4 by a discussion of the implications of these results.

### 2. NOISE ASSESSMENT

Helioseismic holography (hereafter HH) is a method which computationally extrapolates the surface acoustic field into the solar interior (Lindsey & Braun 1997, 2000) in order to estimate the amplitudes of the waves propagating into and out of a focus point at a chosen depth and position in the solar interior. The magnitudes and phases of these amplitudes, called the ingression and egression, are used to detect flows and other perturbations to the waves. The method employed for horizontal flow diagnostics is based on the egressions and ingressions computed in the *lateral vantage* employing pupils spanning four quadrants extending in the east, west, north, and south directions from the focus (Braun et al. 2004, 2007; Lindsey & Braun 2004). In the lateral vantage, the  $p$ -modes sampled by the pupil propagate through the focal point in directions inclined up to  $\pm 45^\circ$  from the direction parallel to the surface (see Fig. 3 of Braun et al. 2007). A difference in the travel times between waves traveling from one pupil to its opposite and waves traveling in the reverse direction is produced by flows along the path of the waves. In particular, the travel-time differences,  $\delta\tau_{ew}$  and  $\delta\tau_{ns}$ , derived from the east-west and north-south quadrant pairs, respectively, provide the HH signatures sensitive to the two components of the horizontal flow. The sign of the

<sup>1</sup> See <http://gong.nso.edu/data> and <http://soi.stanford.edu/data>, respectively.

travel-time difference is such that a northward velocity component will produce a negative value of  $\delta\tau_{\text{ns}}$ . The lateral-vantage geometry samples more than 70% of the wave modes which pass through the focus. The remaining waves, propagating more vertically than the waves appearing in the pupil, are substantially less sensitive to horizontal flows near the focus. Table 1 lists the focus depths and the pupil radii used in this study. The pupil radii are defined from ray theory. The range of (spherical-harmonic) mode degrees ( $\ell$ ) at 4 mHz, selected by each pupil, is also listed in the table. The lower  $\ell$ -value denotes the modes propagating at  $\pm 45^\circ$  from the horizontal direction which propagate through the focus and reach the surface at either the inner or outer pupil radius. The highest  $\ell$ -value listed indicates modes propagating horizontally through the focus. The focus depths extend down to the base of the convection zone. However, the analysis is conceptually similar to previous near-surface measurements (Braun et al. 2007).

Three weeks of full-disk Dopplergrams with 1 minute cadence, obtained from MDI, were used in this study. The data set spans the interval from 1996 June 25 to July 16, and coincides with a period of very low magnetic activity on the Sun. Smaller spans of data at other epochs (2002 March and 2003 October) were also examined. Travel-time maps made at all three epochs exhibit similar noise characteristics, and we show here only the results using the 1996 data. The following steps summarize the general data reduction: (1) a projection of each full-disk Dopplergram onto nine overlapping Postel projections (each extending  $180^\circ \times 180^\circ$ ) centered on grid points separated by  $40^\circ$  in heliographic latitude ( $B$ ) and central meridian distance ( $CMD$ ) referenced to midday and rotating with the Carrington rate, (2) computation of ingress and egress amplitudes for each 24 hr segment of remapped Dopplergrams by a 2D convolution of the data with appropriate Green's functions, (3) computation of the travel-time difference maps, and (4) extraction and remapping of the central  $40^\circ \times 40^\circ$  portion of each of the nine subregions to form a mosaic in heliographic coordinates spanning  $120^\circ \times 120^\circ$  (see Fig. 1). The ingress and egress measurements are described elsewhere (Lindsey & Braun 1997, 2000) and are performed under the eikonal approximation in spherical coordinates. The large size of the overlapping Postel's projected subregions is dictated by the large pupil required for the deepest foci in Table 1. The 2D convolution in step 2 is a time-saving convenience, appropriate for the type of preliminary noise estimates we are interested in, but distorts the resulting travel-time difference maps. This occurs because of a geometrical mismatch between the fixed annular pupil assumed for the convolution operation and the correct pupil whose shape varies with position in the Postel projection. This deviation worsens as the horizontal position of the focus is moved away from the central (tangent) point of the Postel projection, and the effects of this can therefore be constrained by combining maps made using multiple locations of the tangent point. The consequences of this distortion for the results presented here are discussed below.

Figure 1 shows selected maps of the mean  $\delta\tau_{\text{ns}}$  and standard deviation  $\sigma_0$  of the north-south travel-time difference over 20 consecutive (24 hr duration) sets of measurements. The maps for 1 day of data (June 27) were not included in further analysis due to an anomalously high amount of poor images. Near the surface (e.g., Fig. 1a), the meridional flow produces a distinct negative (positive) travel-time difference in the north (south) hemisphere. As the focus depth increases, this signature becomes less visible. A distinct pattern at high latitudes is also evident and increases significantly with greater focus depth.

TABLE 1  
PUPIL SIZE AND MODE DEGREES

Depth (Mm)	Pupil Radii (deg)	$\ell$ at 4 mHz
30	1.3–10.5	166–235
37	1.7–12.9	145–205
45	2.0–15.4	128–180
54	2.4–18.2	113–159
64	2.9–21.1	100–142
76	3.4–24.1	89–127
88	4.0–26.5	81–114
100	4.5–29.2	73–104
114	5.2–32.0	66–93
130	5.9–35.2	59–84
150	6.8–41.4	52–74
170	7.7–48.1	46–66
190	8.6–54.9	41–58
200	9.1–57.1	39–55

This pattern is opposite in sign of the meridional signature and is clearly an artifact centered on the position of disk center ( $CMD, B$ ) = ( $0^\circ, 3^\circ$ ) which are as observed by MDI. An examination of maps of the east-west travel-time difference (not shown) reveals that this artifact takes the form of a “flow” converging from all directions toward disk center.

Remarkably, the maps of the standard deviation (Figs. 1d–1f) indicate that, apart from the vicinity of the solar limb, the noise for a single travel-time measurement is fairly constant ( $\sigma_0 \approx 4$  s) with focus depth. There is a granularity in these maps which becomes coarser with depth and is related to the increase in the horizontal wavelength of the modes used to make the measurements. An increase in the standard deviation near the solar limb is evident. In addition, there is a noticeable excess of  $\sigma_0$  near positions ( $CMD, B$ ) = ( $\pm 20^\circ, \pm 20^\circ$ ) which are the corners of the individual subregions of the mosaic. The noise in these corners is about 15% above the values near the Postel tangent points for all focus depths used here. This feature likely results from the use of the 2D convolution of Postel's projections described earlier.

Due to signal-to-noise issues we assume any current or future attempt to deduce properties of the deep meridional circulation will make use of longitudinal averaging and very likely also involve at least modest smoothing in latitude. Figures 1g–1i show how the standard deviation of the average over  $CMD$  of  $\delta\tau_{\text{ns}}$  (red lines) is reduced in comparison with the standard deviation of  $\delta\tau_{\text{ns}}$  along a single longitude (blue lines). Figure 2 shows the standard deviation ( $\sigma_a$ ) of averages of  $\delta\tau_{\text{ns}}$  over strips spanning  $120^\circ$  in  $CMD$  and  $15^\circ$  in  $B$ . Unlike the standard deviation ( $\sigma_0$ ) corresponding to specific horizontal focus positions which show little or no variation with focus depth, the standard deviation of the mean ( $\sigma_a$ ) increases with depth at all latitudes. This is a consequence of having fewer independent measurements within a fixed area as the depth increases and is analogous to the common problem in global helioseismology of having fewer modes with which to deduce either structural perturbations or flows at greater depths within the Sun. There is also an increase in noise for measurements at high latitudes, consistent with the maps of  $\sigma_0$  (Fig. 1). Significantly, the values of  $\sigma_a$  for the  $15^\circ$ – $30^\circ$  strips are very close to the results for the  $0^\circ$ – $15^\circ$  strip. This offers some assurance that the contribution of noise due to the 2D convolution (which should preferentially influence the  $15^\circ$ – $30^\circ$  strip) does not add substantially to the results shown in Figure 2.

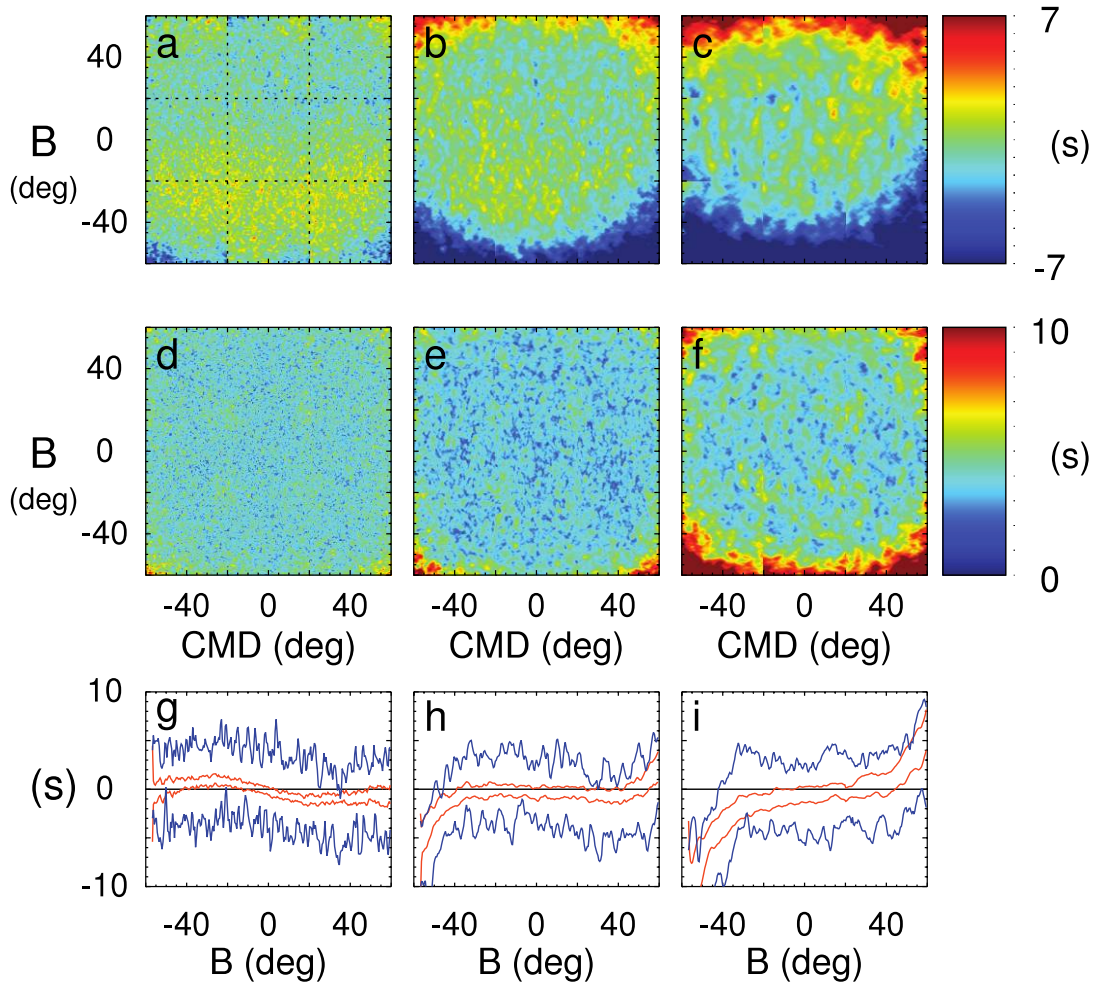


FIG. 1.—Maps of (a–c) the mean and (d–f) standard deviation of north-south travel-time differences for 20 consecutive 24 hr measurements. (g–i) Vertical slices of the mean travel-time difference at  $CMD = 0$  plus or minus the standard deviation (*blue lines*), and a longitudinal average of the travel-time difference plus or minus the standard deviation of the average (*red lines*). From left to right the focus depths of the measurements are 30, 100, and 200 Mm, respectively. The dashed lines in (a) indicate the nine subregions which are Postel projected and analyzed separately to be combined into a larger mosaic.

### 3. FORWARD MODELS

We use both the Born and ray approximations to estimate the travel-time shifts that would be caused by a return flow near the base of the convection zone. For a discussion of the ray approximation see Giles (2000). We used the numerical approach of Christensen-Dalsgaard et al. (1989) for computing ray paths in spherical geometry.

For this Letter we also make rough estimates of the sensitivity of HH travel times to weak, steady, and horizontally uniform flows by approximating the convection zone as a plane-parallel layer. The functions which describe the linear sensitivity of the power spectrum to a horizontally uniform flow can be computed using a generalization of the Born-approximation based approach of Gizon & Birch (2002) and Birch & Gizon (2007). We used the normal-mode summation Green's functions from Birch et al. (2004) although with the eigenfunctions for a spherical Sun in place of those for a plane-parallel version of model S. We used the source model of Birch et al. (2004). Changes in the power spectrum may easily be related to changes in the ingress-egression correlation through the expression for the expectation value of the correlation. The result is a set of sensitivity kernels which relate the correlations (and thus the travel-time shifts) with the flows.

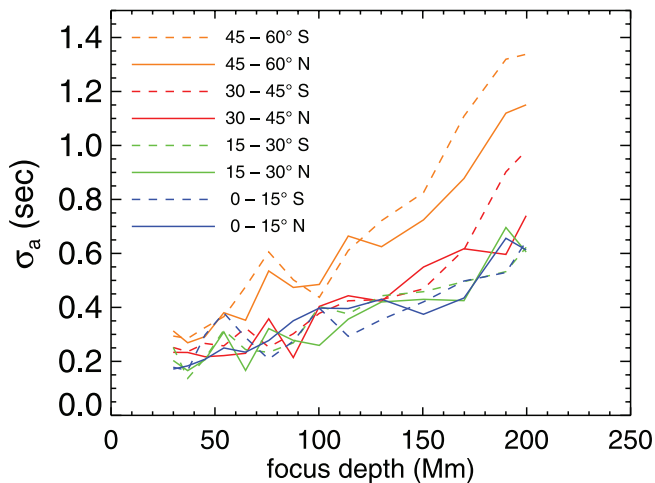


FIG. 2.—Standard deviation (over 20 consecutive 24 hr measurements) of the mean north-south travel-time difference averaged over a strip of the Sun spanning  $15^\circ$  in latitude and  $120^\circ$  in central meridian distance. Different colors indicate different latitudes of the center of the strip, while solid (dashed) lines indicate the southern (northern) hemisphere. In general, the mean standard deviation increases with the depth of the focus, and also increases at high latitudes.

Using the sensitivity functions we estimate the travel-time shifts caused by deep return flows of the form  $v(z) = A \cos[\pi(r - r_c)/2\Delta r]$  for  $r_c < r < r_c + \Delta r$  and  $v(z) = 0$  otherwise. Here  $r_c = 496$  Mm is the radius of the base of the convection zone,  $\Delta r$  is the thickness of the return flow, and  $A$  is the maximum amplitude of the flow (Giles' model B can be roughly approximated with  $A \approx 3$  m s<sup>-1</sup> and  $\Delta r \approx 60$  Mm). Figure 3 shows travel-time differences, for two focus depths, as a function of  $\Delta r$ , predicted from the two methods. It is noteworthy that the times computed under the Born approximation can differ substantially from those predicted by the ray approximation; this difference depends on the functional form of the flow as well as the focus depth. Much of the sensitivity in the Born approximation lies below the lower turning point of the corresponding ray. In addition, for a sufficiently thick return flow the Born travel-time shifts are greater for the shallower focus depth than for the deeper focus depth. The deeper measurements use waves of higher phase speed, which undergo a smaller phase shift in a horizontally uniform flow. For the purposes of this Letter, either approximation appears reasonable.

#### 4. DISCUSSION

To estimate the amount of data needed for a detection of the return flow, we conservatively assume that a successful detection requires a signal-to-noise ratio of 3 for travel-time measurements near the base of the convection zone. Thus for the types of return flows shown in Figure 2, we require a measurement precision on the order of 0.01 s. Given a random noise of 0.6 s for a single day for a HH measurement over a 15° strip (Fig. 2), it is apparent that a lower limit of around 12 years of uninterrupted data is needed for a detection of a mean return flow with characteristics similar to Giles' model B using a travel-time shift of 0.027 s (i.e., the larger of the two estimates), while the more confined flows to the left of the vertical line in Figure 3 would require on the order of hundreds of years.

These estimates are derived assuming the error in the mean travel-time shifts decreases with the square root of the length of the time series (Gizon & Birch 2004). This assumption was validated by measuring the decrease of the standard deviation, assessed within a circular area near disk center, of the travel-time shifts averaged over  $N$  days as  $N$  was increased from 1 to 20. Combining data from both hemispheres and sacrificing some latitudinal resolution (e.g., to 30°) it should be possible to (roughly) halve the required duration. We therefore tentatively conclude that a 3  $\sigma$  detection of a return flow of a magnitude similar or smaller than Giles' model B is possible only with an amount of data comparable or greater than a solar cycle.

The additional noise contributions or systematic errors due to analysis artifacts or details of the modeling procedures are not considered here, so that the results represent a "best case" scenario. We anticipate that high-quality measurements spanning a range of depths will actually be needed to construct a model of the flow. Our emphasis on the signal-to-noise ratio of the individual measurements is based on the relative "completeness" of lateral-vantage HH in that a single ingress-egression correlation efficiently samples and combines most of the waves propagating through a particular depth. We therefore assume that the uncertainty in the inferred flow at the base of the convection zone will be dominated by the random noise contribution to measurements focused at that position.

It is worthwhile to compare our results with uncertainties in

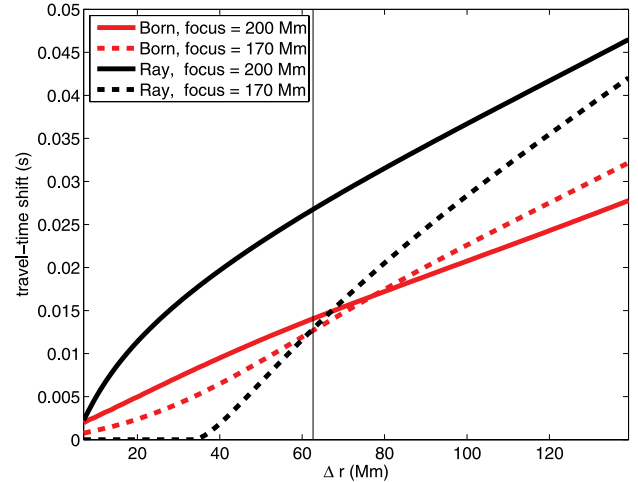


FIG. 3.—Expected north-south travel-time difference as functions of the width of a hypothesized meridional return flow at the base of the convection zone with a peak value of 3 m s<sup>-1</sup> (see text). The flow is set to zero in the radiative zone. The red (black) lines show the results of a Born (ray) approximation calculation, and the solid (dashed) lines show the results for focus depths of 200 (170) Mm below the surface. The vertical line indicates the width which roughly corresponds to Giles' model B.

other helioseismic measurements of flows near the base of the convection zone. First, our results are consistent with the ambiguous results of Giles (2000), namely his failure to distinguish a model with a return-flow component from a model without this component, since we estimate that the 792 days of data he employed would provide only about a 1  $\sigma$  assessment of the return component of model B. Second, our results are consistent with uncertainties in zonal flows found at similar depths. From inversions of global-mode frequency splittings, for example, Howe et al. (2000) derive 1  $\sigma$  errors of inverted rotation rates at a depth of 195 Mm of about 1 nHz (corresponding to 4.4 m s<sup>-1</sup>) for 72 day sets of MDI observations with an averaging kernel approximately 50 Mm wide (FWHM) in depth and about 15° wide in latitude. A 3  $\sigma$  detection of an average 1.5 m s<sup>-1</sup> zonal flow over this range in depth and latitude would therefore require about 15 years of frequency-splitting measurements which agrees very well with the estimate presented here. The consistency of our results with other measurements suggests that the uncertainties introduced by solar realization noise are likely a major limitation to all helioseismic methods.

Although direct measurements of temporal variability of the return component over timescales equal to or less than a solar cycle appear unlikely, we note that some inferences about variability could be made using shallower flow measurements and assuming mass conservation, as did Giles (2000). Regardless of possible temporal variability, it is likely well worth the effort to carry out analyses and modeling of existing decade-length helioseismic observations to either detect or constrain the mean return component. However, we note that there are a considerable number of potential qualifications to the rather simple estimates derived here. Some of these involve issues of the resolution of the models (e.g., the ability to infer the existence of multiple meridional cells or sharp gradients of flow in latitude or depth). In addition, we expect considerable challenges to the probing of any flows in the deep convection zone raised by the need to understand and remove possible artifacts and systematic effects. Some of these effects are visible as system-

atic differences between inferred flows using separate but contemporary data sets (González Hernández et al. 2006). These differences are often of the order of a few  $\text{m s}^{-1}$  which, while troublesome for probing even the near-surface layers, are clearly disastrous for the unambiguous identification of a return flow of comparable or smaller magnitude. The critical need for multiple sources of long-duration helioseismic observations combined with careful artifact identification and correction pro-

cedures in reducing both systematic effects and random noise should be clear.

We appreciate useful discussions with M. Woodard. D. C. B. and A. C. B. are supported by funding through NASA contract NNN05CC76C and NSF grant AST 04-06225, and a subcontract through the NASA sponsored HMI project at Stanford University awarded to NWRA.

## REFERENCES

- Birch, A. C., & Gizon, L. 2007, *Astron. Nachr.*, 328, 228  
 Birch, A. C., Kosovichev, A. G., & Duvall, T. L., Jr. 2004, *ApJ*, 608, 580  
 Braun, D. C., Birch, A. C., Benson, D., Stein, R. F., & Nordlund, Å. 2007, *ApJ*, 669, 1395  
 Braun, D. C., Birch, A. C., & Lindsey, C. 2004, in *Proc. SOHO 14/GONG 2004 Workshop: Helio- and Asteroseismology: Towards a Golden Future*, ed. D. Danesy (ESA SP-559; Noordwijk: ESA), 337  
 Braun, D. C., & Fan, Y. 1998, *ApJ*, 508, L105  
 Chou, D.-Y., & Ladenkov, O. 2005, *ApJ*, 630, 1206  
 Choudhuri, A. R., Schussler, M., & Dikpati, M. 1995, *A&A*, 303, L29  
 Christensen-Dalsgaard, J., Thompson, M. J., & Gough, D. O. 1989, *MNRAS*, 238, 481  
 Dikpati, M., & Gilman, P. A. 2007, *Sol. Phys.*, 241, 1  
 Giles, P. M. 2000, Ph.D. thesis, Stanford Univ.  
 Giles, P. M., Duvall, T. L., Jr., Scherrer, P. H., & Bogart, R. S. 1997, *Nature*, 390, 52  
 Gizon, L., & Birch, A. C. 2002, *ApJ*, 571, 966  
 ———. 2004, *ApJ*, 614, 472  
 Glatzmaier, G. A., & Gilman, P. A. 1982, *ApJ*, 256, 316  
 González Hernández, I., Komm, R., Hill, F., Howe, R., Corbard, T., & Haber, D. A. 2006, *ApJ*, 638, 576  
 González Hernández, I., Patrón, J., Bogart, R. S., & the SOI Ring Diagram Team. 1999, *ApJ*, 510, L153  
 Haber, D. A., Hindman, B. W., Toomre, J., Bogart, R. S., Larsen, R. M., & Hill, F. 2002, *ApJ*, 570, 855  
 Hathaway, D. H. 1996, *ApJ*, 460, 1027  
 Hathaway, D. H., Nandy, D., Wilson, R. M., & Reichmann, E. J. 2003, *ApJ*, 589, 665  
 Howe, R., Christensen-Dalsgaard, J., Hill, F., Komm, R. W., Larsen, R. M., Schou, J., Thompson, M. J., & Toomre, J. 2000, *Science*, 287, 2456  
 Hughes, S. J., & Thompson, M. J. 2003, in *Proc. SOHO 12/GONG +2002: Local and Global Helioseismology: The Present and Future*, ed. H. Sawaya-Lacoste (ESA SP-517; Noordwijk: ESA), 307  
 Lindsey, C., & Braun, D. C. 1997, *ApJ*, 485, 895  
 ———. 2000, *Sol. Phys.*, 192, 261  
 ———. 2004, *ApJS*, 155, 209  
 Roth, M., & Stix, M. 2008, *Sol. Phys.*, 251, 77  
 Scherrer, P. H., et al. 1995, *Sol. Phys.*, 162, 129  
 Schou, J. 2003, *ApJ*, 596, L259  
 Wang, Y.-M., Sheeley, N. R., Jr., & Nash, A. G. 1991, *ApJ*, 383, 431  
 Zhao, J., & Kosovichev, A. G. 2004, *ApJ*, 603, 776